ROLE OF CLUSTERIZATION ALGORITHMS IN MULTIFRAGMENTATION OF MASS ASYMMETRIC REACTIONS

Dr. Supriya Goyal
PG Department of Physics, GSSDGS Khalsa College, Patiala-147001, India
Email: ashuphysics@gmail.com

Abstract:
In this paper, we studied the effect of clusterization algorithms (fragment formation techniques) on the phenomenon of multifragmentation for mass asymmetric central reactions using quantum molecular dynamics model. We simulated the reactions for *η(mass asymmetry parameter)* = 0-0.74 at E = 20-200 MeV/nucleon and using *MSTB(2.1)* and *SACA(2.1)* (minimum spanning tree and simulated annealing clusterization algorithms with microscopic binding energy cut, respectively). Our results clearly indicates that both SACA(2.1) and MSTB(2.1) methods explain the experimental results nicely, therefore, like for symmetric reactions one can also use the most simplified MSTB(2.1) algorithm for mass asymmetric reactions to get the most stable and bound fragments as compared to most complicated SACA versions.

Keywords- Heavy-Ion collisions, Mass Asymmetry, Clusterization algorithms, Quantum Molecular Dynamics Model
DOINumber: 10.48047/nq.2022.20.2.NQ22383 NeuroQuantology2022;20(2):837-846

1. Introduction

In the past few years, various experimental and theoretical studies have been conducted to investigate multifragmentation in heavy ion collisions. These studies have covered both symmetric and asymmetric reactions [1-15]. The reaction's mass asymmetry can be expressed as $\eta = (A_T - A_P / A_T + A_P)$; where A_P and A_T denote the mass of the projectile and target, respectively. Mass asymmetric reactions are indicated by non-zero values of η, while symmetric reactions by $\eta=0$. Because a large portion of the excitation energy in symmetric reactions results in greater compression, mass asymmetric reactions lack compression but have thermal energy [16-18]. *FOPI* collaborations conducted the study on Ca+Au/Au+Ca asymmetric systems at 1.5 GeV/nucleon for the sidewards flow, the squeeze out, and the nuclear stopping; both in the normal and inverse kinematics [6]. Moreover, *Kaos* group has shown the emission of kaons and pions in the mass asymmetric reactions at high energies [7]. The preferential emission of fragments and pions in mass asymmetric nucleus-nucleus collisions has also been studied [8]. It has also been found that sub-barrier fusion has enhanced magnitude at low incident energies for large mass asymmetric systems [19]. In intermediate energy range, the energy of maximum production of IMFs (intermediate mass fragments) decreases linearly with η [2]. At relativistic

energies, experimental work on mass asymmetric reactions is done by FASA, PHENIX and ISIS collaborations [2,20]. On the theoretical front, Kaur *et al.* has studied the effect of η on the multiplicity of IMFs, nuclear stopping, transition energy by keeping total system mass constant [9]. Goyal *et al.* has seen η effect on geometry (upto 62%) and energy (upto 40%) of vanishing flow [21]. In other study, the effect of input and output parameters on O+Ag/Br reactions have been seen in Ref. [13, 14]. To study the alpha structure of ^{16}O, Guo *et al.* studied ^{16}O +^{197}Au reaction at 40 MeV/nucleon [22]. Sharma *et al.* [23] did a detail comparison of theoretical calculations with experimental data of nearly symmetric and asymmetric reactions and found that at extreme lower and higher incident energies, results deviate from experimental data for asymmetric reactions. Also, Sood *et al.* [24] have noticed the role of η on fragment emission, entropy production and critical behavior. In a similar way, many different studies are reported on experimental as well as theoretical front, that contain reactions of ^{197}Au+^{12}C, ^{58}Ni+^{12}C, ^{64}Zn+^{27}Al, ^{20}Ne+^{12}C, ^{20}Ne +^{27} Al, ^{20}Ne +^{63} Cu, ^{40}Ar +^{207} Pb, ^{12}C +^{197} Au, and ^{1}H +^{197} Au etc. [3–14]. A study using different clusterization for symmetric reactions has been performed in detail in Ref. [15]. It has been shown in Ref. [3,14,25] that the QMD+MST calculations successfully explain the multifragmentation at low energy central collisions but fails badly for reactions with non-zero values of η. This is because of the absence of proper thermodynamical properties, which play an important role for mass asymmetric reactions, in the models used. While, for symmetric systems, no significant role of model's thermodynamical properties is there. However, MST method was also improved time to time by implementing momentum cuts and energy minimization techniques [25,26] but the results were far from experimental data. Therefore, effects of various clusterization algorithms on multifragmentation for different mass asymmetric colliding nuclei and comparison with experimental data will be done in this study. Section 2 includes the models used for the present study. Section 3 presents the results and discussion with conclusion in Sec. 4.

2. Model

In QMD (n-body) model (details in Ref. [27]), Hamilton's equations are used by each nucleon to follow classical trajectory. The clusterization algorithms then takes QMD generated phase space as input. The spatial correlation approach, i.e. MST [27] method identify fragments with nucleons having internucleon distance less than 4 fm.

In MSTB(1.1) [13,28], 4 MeV/nucleon binding energy cut is employed on fragments (A≥3). But more realistic approach is to apply the energy cut as given in Ref. [29]:

$$E_{bind}^{BWM} = a_v N_f - a_s N_f^{\frac{2}{3}} - a_c \frac{N_f^z\left(N_f^z-1\right)}{N_f^{\frac{1}{3}}} - a_{sym} \frac{\left(N_f-2N_f^z\right)^2}{N_f\left(1+e^{\frac{N_f}{17}}\right)} + \delta_{new}$$

The values of free parameters are given in Ref. [29]. The pairing term δ_{new} is given by:

$$\delta = +a_p N_f^{-\frac{1}{2}}\left(1-e^{\frac{-N_f}{30}}\right) for\ even\ N_f^n - even\ N_f^z,$$

$$\delta = -a_p N_f^{-\frac{1}{2}} \left(1 - e^{\frac{-N_f}{30}}\right) for\ odd\ N_f^n - odd\ N_f^z,$$
$$\delta = 0\ for\ odd\ N_f\ nuclei,$$

With a_p = 12 MeV. This version is named as MSTB(2.1) [15]. Similarly, the extension of SACA(1.1) [25] is named as SACA(2.1) [30]. Moreover, constant binding energy cut is also not realistic. Therefore clusterization methods used in the present study are MSTB(2.1) and SACA(2.1).

3. Results and Discussion

The central reactions of η=0, 0.21, 0.46, 0.67 and 0.74 corresponding to $^{197}Au + ^{197}Au$, $^{129}Xe + ^{197}Au$, $^{40}Ar + ^{108}Ag$, $^{16}O + ^{80}Br$, and $^{16}O + ^{108}Ag$ respectively, are simulated for energy range 20-200 MeV/nucleon using standard energy dependent cugnon cross-section and soft equation of state. As experimental data is available for these reactions, therefore, these reactions are selected for the present study. MSTB(2.1) and SACA(2.1) fragment formation algorithms are used to make clusters with final time as 250 fm/c for MSTB(2.1) and T_{min} for SACA(2.1). The time at which heaviest fragment attains first minimum is taken as T_{min} and its value changes with change in η and incident energy.

Fig. 1 displays the multiplicities per nucleon (i.e. reduced) verses time of $<A^{max}>$, light charged fragments (LCP's), fragments with mass = 4, free nucleons, as well as fragments with masses 5≤A≤9, 3≤A≤14, 5≤A≤48, and 5≤A≤65 for the central reactions at 100 MeV/nucleon with η = 0, 0.46 and 0.74 using SACA(2.1) and MSTB(2.1). To see the effect of η, 'reduced' multiplicities have been used. Figure clearly show that free nucleons and various fragments are the products of excited compound nucleus. Therefore, during the fall of $<A^{max}>$ in the time interval of 20-50 fm/c, a rise in multiplicity of various fragments is seen. As soon as $<A^{max}>$ saturates, the multiplicity of various fragments also saturates with time. One also notices that, due to the decrease in the destruction with η, the size of $<A^{max}>$ show an increase with increase in η of reaction. Obviously, fragment multiplicities display the opposite behavior. The trend is same for SACA(2.1) and MSTB(2.1) but their effect on the multiplicity of various fragments is clearly seen at high compression stages.

In Fig. 2, reduced multiplicities at final time verses incident energy for SACA(2.1) and MSTB(2.1) and for η = 0, 0.46 and 0.74 is shown. The size of $<A^{max}>$ decreases for all η as energy increases whereas opposite behavior is seen for other fragments as the increase in incident energy leads to enhanced nucleon-nucleon collisions. At all incident energies, $<A^{max}>$ size increases with rise in mass aymmetry, while the opposite happens for other multiplicities. More fragments are emitted as the matter shifts to participant area due to enhanced compression in symmetric reactions. The above effect of η on the reduced multiplicities is much clear with MSTB(2.1) clusterization algorithm. With SACA(2.1), the variation of reduced multiplicities with incident energy is nearly same for η = 0 and 0.46, while this is not the case with MSTB(2.1).

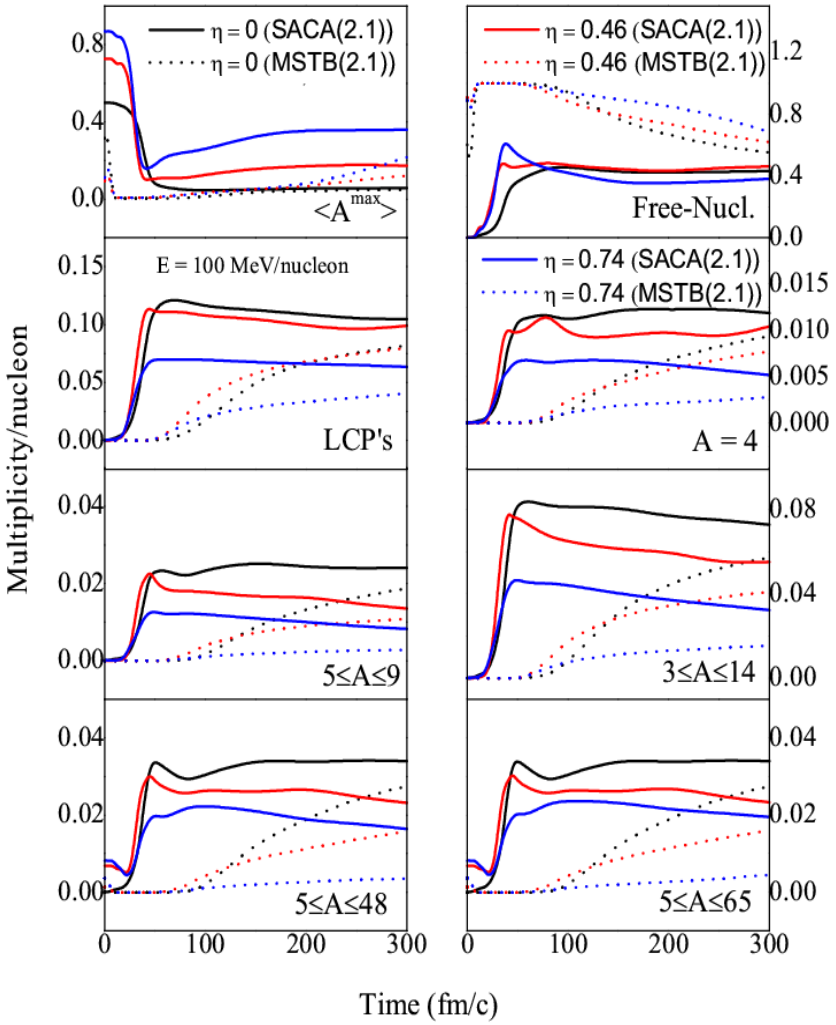

Fig. 1: The time evolution of reduced multiplicities for η = 0, 0.46 and 0.74. Comparison has been shown with SACA(2.1) and MSTB(2.1).

Fig. 3 displays the reduced multiplicities (at final time) using SACA(2.1) and MSTB(2.1), as a function of η at 20, 100, and 200 MeV/nucleon. As η increases, n-n collisions and participant region decreases, therefore, $<A^{max}>$ size increases and other fragment multiplicities decreases. At all asymmetries, at low energies, $<A^{max}>$ is more and decreases with rise in energy. Whereas, LCP's, A = 4 fragments, free nucleons, and 3≤A≤14 show opposite trend. The heavy fragments i.e. 5≤A≤9, 5≤A≤48 and 5≤A≤65 show decreased multiplicity with rise in energy similar to $<A^{max}>$ as they can only survive in the low excitation region. The multiplicity of heavy fragments decreases with rise in η because the heaviest fragment size increases with η and goes beyond the upper range of heavy fragments. The similar trend is also seen with MSTB(2.1) and at higher η the variation in multiplicities of various fragments with incident energy also vanished.

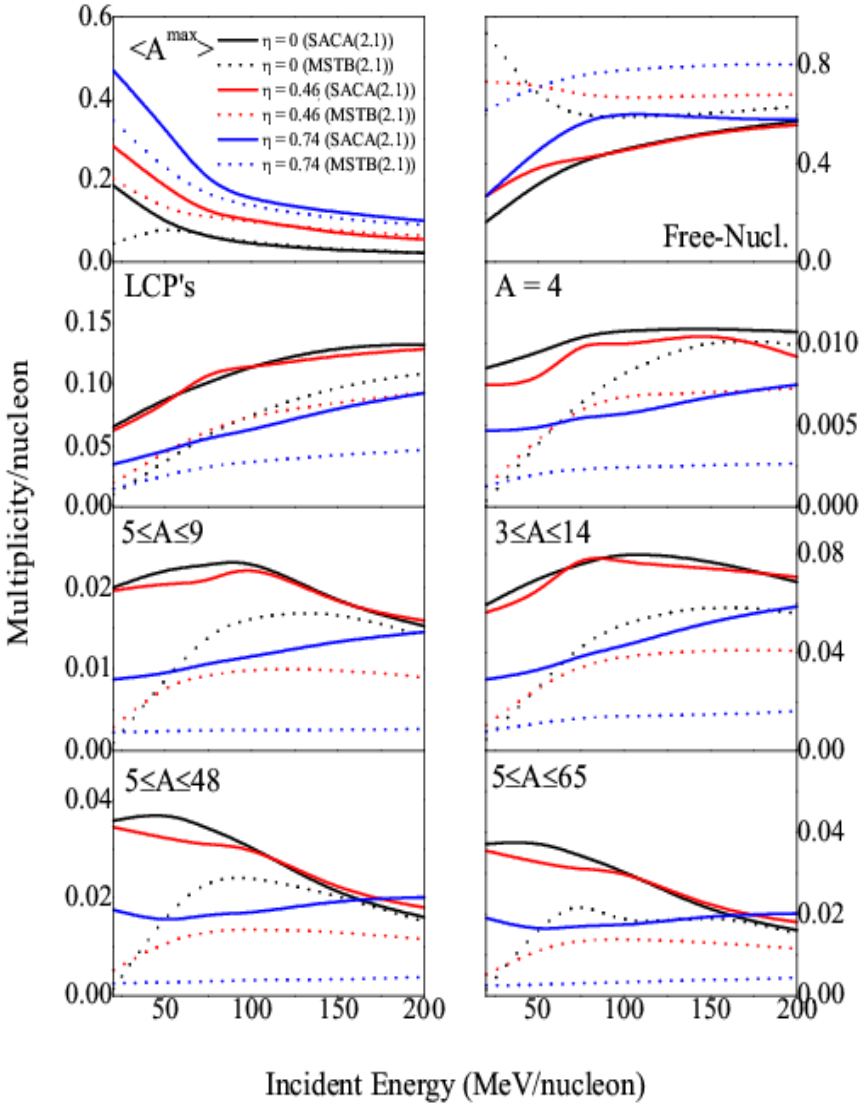

Fig. 2: The reduced multiplicities (at final time) verses incident energy for η = 0, 0.46 and 0.74. Comparison has been shown with SACA(2.1) and MSTB(2.1).

We display in Figs. 4 and 5, normalized charge particle yields (dN/dZ_f) verses fragments charge (Z_f). In Fig. 4, central reaction of ^{16}O+^{108}Ag is analyzed at E = 50, 75, 100, 150, 200 MeV/nucleon. Similarly, in Fig. 5, central reaction of ^{16}O +^{80} *Br* is displayed.

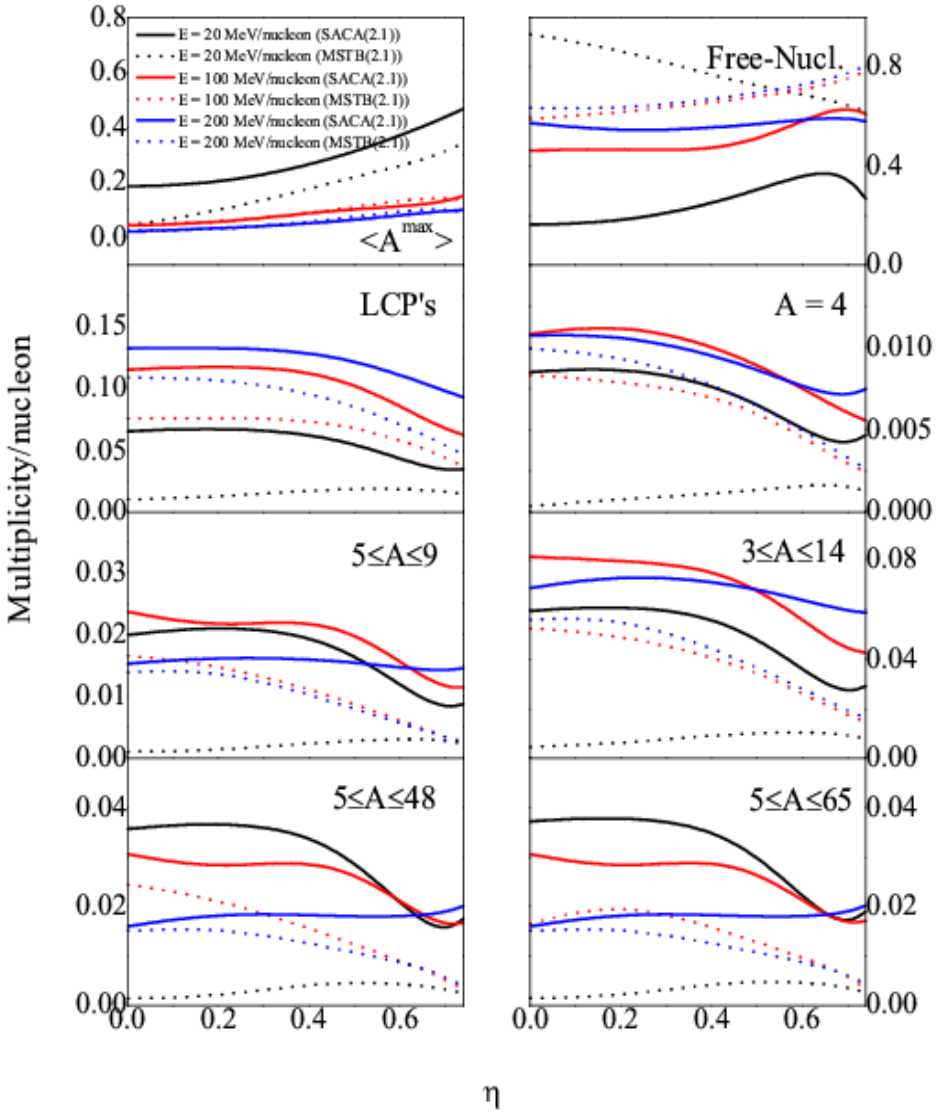

Fig. 3: The reduced multiplicities (at final time) verses η for E = 20, 100 and 200 MeV/nucleon. Comparison has been shown with SACA(2.1) and MSTB(2.1).

While presenting the comparison, one should keep in the mind that (i) among all the events in emulsion experiments, 10% highest were selected. (ii) no impact parameter window was determined experimentally, so while comparing with the data all theoretical attempts take b = 0 fm (iii) as below 0.5 MeV/nucleon kinetic energy, fragments cannot be detected properly, therefore, threshold detection is less than it. In both the figures, at all values of E, our results are close to experimental data [3]. As noticed in Ref. [13, 14], the agreement can be improved if one includes either large n-n cross-section or MDI i.e. momentum (M) dependent (D) interactions (I). Both figures clearly depict that, at low E, we have components consisting of heavy fragment and other associated with the light fragments. As we go to the higher incident energies, one sees disassembly of the system. In between these two limits, fusion-fission transition to phenomenon of multifragmentation is seen.

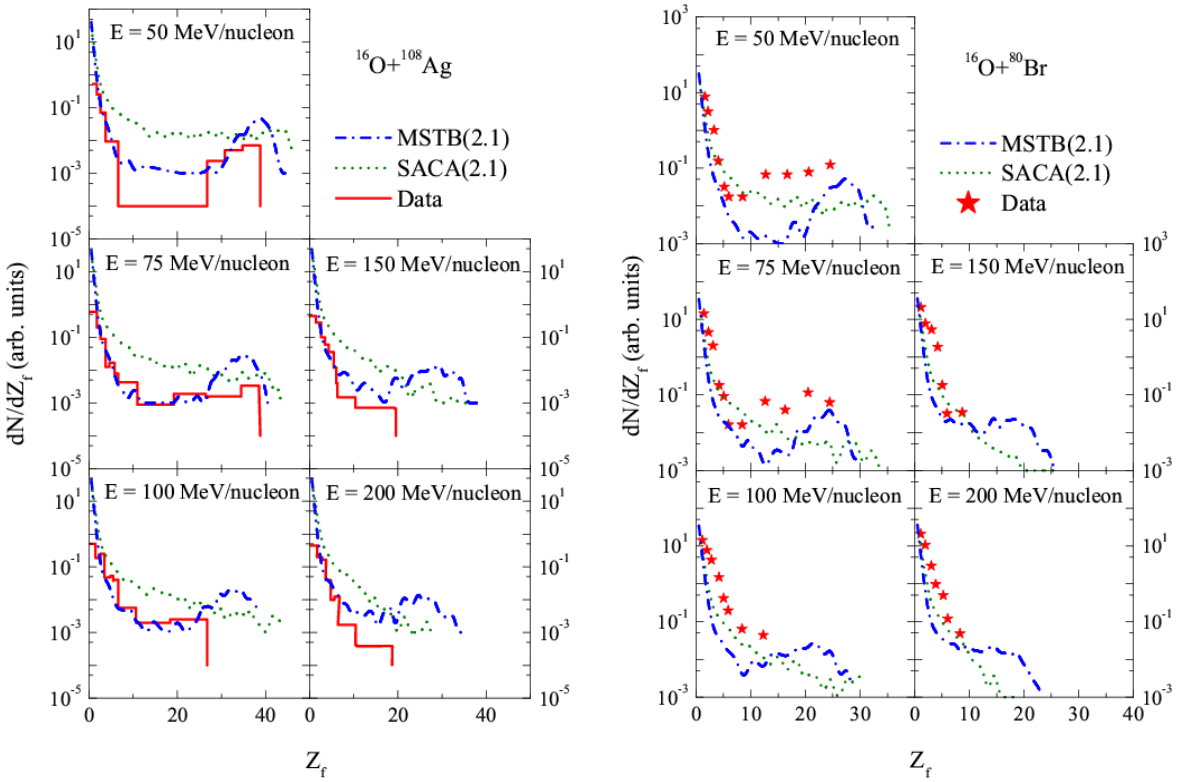

Fig. 4 and 5: The normalized charge distribution for the ^{16}O +^{108}Ag (left) and ^{16}O +^{80} Br (right). The displayed results are at freeze out times. Here data is taken from Ref. [3].

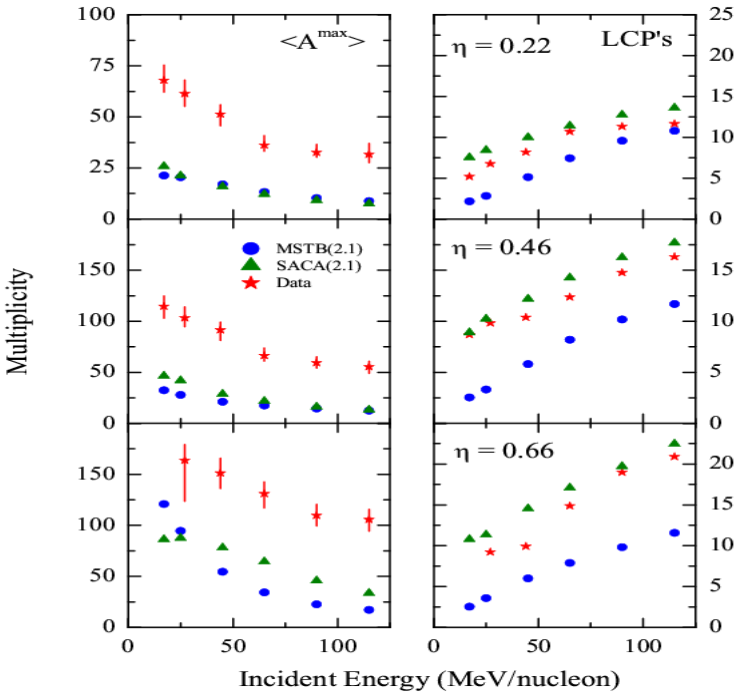

Fig. 6: The size of $< A^{max} >$ (left column) and multiplicity of LCP's (right column) as a function of incident energy for η = 0.22, 0.46, and 0.66. The results are represented by

solid circles (MSTB(2.1)) and solid triangles (SACA(2.1)). Solid stars represents data taken from Ref. [4].

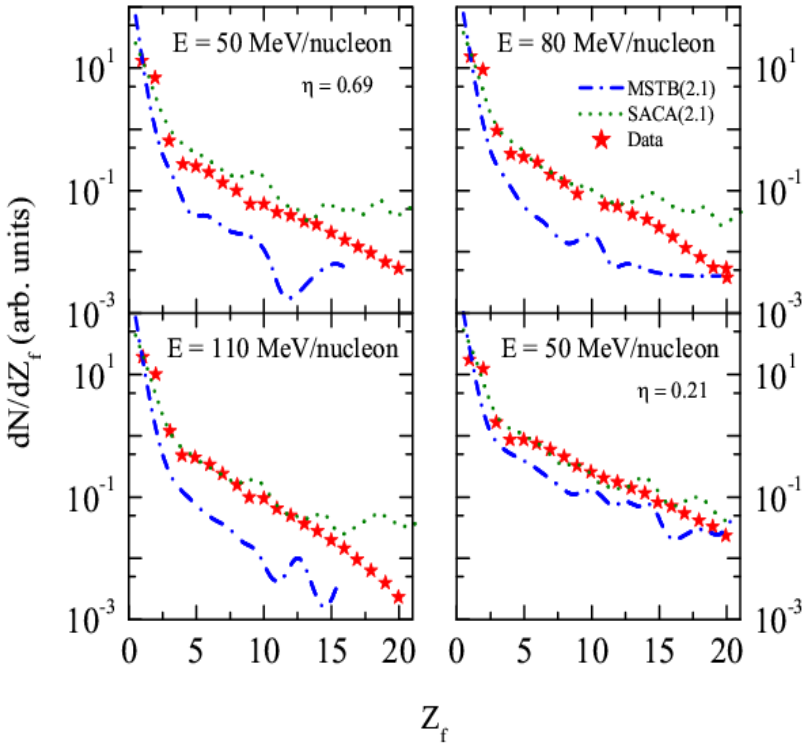

Fig. 7: The charge distribution for η = 0.69 at E = 50-110 MeV/nucleon and η = 0.21 at 50 MeV/nucleon. The solid-dashed line denotes the results with MSTB(2.1) and short-dashed line is with SACA(2.1). Solid stars represent data taken from Ref. [5].

In Fig. 6, we display the size of $<A^{max}>$ formed and LCP's verses incident energy. The results are for η = 0.22, 0.46 and 0.66. Ref. [4] is used for experimental data. The match with data for $< A^{max} >$ is not found in our present study whereas for LCP's, the SACA(2.1) matches with experimental results quite nicely.

In Fig. 7, charge distribution for η = 0.69 and 0.21 at E = 50-110 MeV/nucleon and 50 MeV/nucleon, respectively is displayed. We clearly see from the figure that the results with SACA(2.1) matches nicely with the experimental data [5]. For η = 0.21, even the results with MSTB(2.1) are close to experimental data.

4. Conclusion

Here effect of clusterization algorithms on multifragmentation phenomenon is analyzed for different mass asymmetric reactions. The system size effects were counterbalanced by scaling all the observables with total mass as it was not fixed for different mass asymmetric reactions. The clusterization algorithms used for present study were SACA(2.1) and MSTB(2.1). Our results clearly indicate the significant role of mass asymmetry on reaction dynamics as fragment multiplicities show a

considerable decrease with the increase in η at all incident energies in range of 20-200 MeV/nucleon. The fall in participant area with η is the reason behind this trend. Comparison with experimental data is also displayed. It has been seen that both SACA(2.1) and MSTB(2.1) methods explain the experimental results nicely, therefore, like for symmetric reactions, one can also use the most simplified MSTB(2.1) algorithm for mass asymmetric reactions to get the most stable and bound fragments as compared to most complicated SACA versions.

5. References

[1] J. Hubele *et al.*, Z. Phys. A **340**, 263 (1991); T. Li *et al.*, *ibid.* **70**, 1924 (1993); K. Hagel *et al.*, *ibid.* **68**, 2141 (1992); G. F. Peaslee *et al.*, Phys. Rev. C **49**, R2271 (1994); C. Williams *et al.*, *ibid.* **55**, R2132 (1997); N. T. B. Stone *et al.*, Phys. Rev. Lett. **78**, 2084 (1997); C. A. Ogilvie *et al.*, Phys. Rev. Lett. **67**, 1214 (1991).

[2] M. Begemann-Blaich *et al.*, Phys. Rev. C **48**, 610 (1993); A. Schuttauf *et. al.*, Nucl. Phys. A **607**, 457 (1996).

[3] B. Jakobsson *et al.*, Nucl. Phys A **509**, 195 (1990); H. W. Barz *et al.*, *ibid.* **548**, 427 (1992).

[4] Rulin Sun *et al.*, Phys. Rev. C **61**, 061601(R) (2000) and references therein.

[5] W. G. Lynch, Nucl. Phys. A **545**, 199c (1992).

[6] K. J. Eskola, Nucl. Phys. B **323**, 37 (1989); O. Hartmann, Dissertation, TU Darmstadt (2003).

[7] A. Schmah *et al.*, Phys. Rev. C **71**, 064907 (2005).

[8] H. Stocker, J. A. Maruhn and W. Greiner, Phys. Rev. Lett. **44**, 725 (1980); J. Gosset *et al.*, *ibid.* **62**, 1251 (1989); B. A. Li, W. Bauer and G. F. Bertsch, Phys. Rev. C **44**, 2095 (1991).

[9] V. Kaur and S. Kumar, Phys. Rev. C **81**, 064610 (2010); V. Kaur, S. Kumar and R. K. Puri, Phys. Lett. B **697**, 512 (2011).

[10] D. R. Bowman *et al.*, Phys. Lett. B **189**, 282 (1987); A. Bonasera and L. P. Csernai, Phys. Rev. Lett. **59**, 630 (1987); G. F. Bertsch, W. G. Lynch and M. B. Tsang, Phys. Lett. B **189**, 384 (1987); W. K. Wilson *et al.*, Phys. Rev. C **43**, 2696 (1991); Z. Y. He *et al.*, Nucl. Phys. A **598**, 248 (1996); J. A. Hauger *et al.*, Phys. Rev. Lett. **77**, 235 (1996); R. Sun *et al.*, *ibid.* **84**, 43 (2000); S. P. Avdeyev *et al.*, Phys. Lett. B **503**, 256 (2001).

[11] D. Beavis *et al.*, Phys. Rev. C **45**, 299 (1992); S. R. Souza and C. Ngo, *ibid.* **48**, R2555 (1993); B. A. Bian, F. S. Zhang and H. Y. Zhou, Nucl. Phys. A **807**, 71 (2008).

[12] R. E. Renfordt *et al.*, Phys. Rev. Lett. **53**, 763 (1984); Q. Pan and P. Danielewicz, *ibid.* **70**, 2062 (1993); M. J. Huang *et al.*, *ibid.* **77**, 3739 (1996); J. Chance *et al.*, *ibid.* **78**, 2535 (1997); A. Chernomoretz *et al.*, Phys. Rev. C **65**, 054613 (2002).

[13] S. Kumar and R. K. Puri, Phys. Rev. C **58**, 2858 (1998).

[14] J. Singh and R. K. Puri, J. Phys. G: Nucl. Part. Phys. **27**, 2091 (2001); J. Singh, Ph.D. Thesis, Panjab University, Chandigarh, India (2001).

[15] S. Goyal and R. K. Puri, Phys. Rev. C **83**, 047601 (2011).

[16] S. Leray, C. Ngo, P. Bouissou, B. Remoud and F. Sebille, Nucl. Phys. A **531**, 177 (1991).

[17] S. R. Souza, L. de Paula, S. Leray, J. Nemeth, C Ngo and H. Ngo, Nucl. Phys. A **571**, 159 (1994).

[18] L. Zhuxia, C. Hartnack, H. Stocker and W. Greiner, Phys. Rev. C **44**, 824 (1991).

[19] V. Singh *et al.,* Phys. Lett. B **765**, 99

(2017); V. Tripathi *et al.*, Phys. Rev. C **65**, 014614 (2001); B. A. Bian, F. S. Zhang and H. Y. Zhou, Phys. Lett. B **665**, 314 (2008).

[20] K. Kwiatkowski *et al.,* Phys. Lett. B **423**, 21 (1998); S. P. Avdeyev *et al.,* Eur. Phys. J. A **3**, 75 (1998); S. S. Adler *et al.,* Phys. Rev. Lett. **96**, 0102304 (2006); S. S. Adler *et al.,* Phys. Rev. Lett. **107**, 142301 (2011).

[21] S. Goyal and R. K. Puri, Nucl. Phys. A **853**, 164 (2011); S. Goyal, Nucl. Phys. A **856**, 154 (2011).

[22] C.-C. Guo *et al.,* Phys. Rev. C **99**, 044607 (2019).

[23] A. Sharma *et al.,* Nucl. Phys. A **945**, 95 (2016)

[24] S. Sood *et al.,* Chinese Phys. C **45**, 014101 (2021); S. Sood *et al.*, Phys. Scr. **96**, 015302 (2021).

[25] R. K. Puri, C. Hartnack and J. Aichelin; Phys. Rev. C **54**, R28 (1996); R. K. Puri and J. Aichelin, J. Comp. Phys. **162**, 245 (2000).

[26] Y. G. Ma *et al.,* Phys. Rev. C **51**, 710 (1995); Y. G. *et al.,* Phys. Rev. C **69**, 031604(R) (2004); S. Sood *et al.,* Phys. Rev. C **99**, 054612 (2019); S. Kumar and R. K. Puri, Phys. Rev. C **58**, 320 (1998); J. Singh, S. Kumar and R. K. Puri, Phys. Rev. C **63**, 054603 (2001); R. Kumar *et al.,* Phys. Rev. C **89**, 064608 (2014); R. Kumar, J. Phys. G: Nucl. Part. Phys. **43**, 025104 (2016).

[27] J. Aichelin, Phys. Rep. **202**, 233 (1991).

[28] J. K. Dhawan and R. K. Puri, Eur. Phys. J. A **33**, 57 (2007); Y. K. Vermani and R. K. Puri, J. Phys. G: Nucl. Part. Phys. **36,** 105103 (2009).

[29] C. Samanta and S. Adhikari, Phys. Rev. C **65**, 037301 (2002); C. Samanta and S. Adhikari, Phys. Rev. C **69**, 049804 (2004); C. Samanta and D. N. Basu, Mod. Phys. Lett. A **20**, 1605 (2005).

[30] Y. K. Vermani et al., J. Phys. G: Nucl. Part. Phys. 37, 015105 (2010).